Earth and Planetary Science Letters 505 (2019) 86–95

Contents lists available at ScienceDirect

Earth and Planetary Science Letters

www.elsevier.com/locate/epsl

Beryllium isotope signatures of ice shelves and sub-ice shelf circulation

Duanne A. White [a,*], David Fink [b], Alexandra L. Post [c], Krista Simon [b], Ben Galton-Fenzi [d,e], Simon Foster [a], Toshiyuki Fujioka [b], Matthew R. Jeromson [a], Marcello Blaxell [a], Yusuke Yokoyama [f]

[a] Institute for Applied Ecology, University of Canberra, ACT, 2617, Australia
[b] Australian Nuclear Science and Technology Organisation (ANSTO), PMB 1, Sydney, NSW, 2234, Australia
[c] Geoscience Australia, Symonston, ACT, 2609, Australia
[d] Antarctic Climate Evolution Cooperative Research Centre, Private Bag 80, Hobart, TAS, 7001, Australia
[e] Australian Antarctic Division, Kingston, Tasmania, Australia
[f] Univesity of Tokyo, Tokyo, Japan

ARTICLE INFO

Article history:
Received 14 June 2018
Received in revised form 1 October 2018
Accepted 5 October 2018
Available online 25 October 2018
Editor: D. Vance

Keywords:
meteoric ^{10}Be
marine sediments
Be isotope mixing
sub-ice shelf currents
sediment advection

ABSTRACT

Be isotopes are a useful tracer of sediment source and transport pathways but have not been widely tested in glacio-marine environments. We measured Be isotopes in a range of depositional environments from open marine, sub-ice shelf and subglacial settings throughout Prydz Bay, one of Antarctica's largest ice drainage systems. We find that strong sub-ice shelf and bottom current circulations can advect ^{10}Be-rich open marine sediments into an ice shelf cavity, and ^{10}Be-poor terrestrial sediments onto the continental shelf at the ice shelf outflow, meaning that ^{10}Be concentrations reflect sub-ice shelf circulation patterns rather than depositional environment. However, HCl-extractable ^{10}Be/^{9}Be ratios can provide a more robust discrimination of sediment deposited in open marine and sub-ice shelf settings. Thus, Be isotopes are a useful tracer of both environmental setting and sub-ice shelf circulation strength in both modern and paleo-ice sheet margins.

1. Introduction

Beryllium isotopes display a range of properties that make them useful tracers of geochemical processes and sediment sources. ^{10}Be is produced in the atmosphere (termed meteoric ^{10}Be) by interaction of cosmic rays with oxygen nuclei, and decays with a 1.387-million-yr half-life (Chmeleff et al., 2010). Cosmic rays also interact with Earth surface rocks (termed *in-situ* ^{10}Be), although production rates are orders of magnitude lower. Stable ^{9}Be is a naturally occurring trace element in crustal rocks and accumulates, together with meteoric ^{10}Be, in many sediment archives in either the primary minerals or secondary weathering products (von Blanckenburg et al., 2012).

Much of the development and application of beryllium isotopes in sediment cycling to date has focused on temperate terrestrial and marine environments. In temperate areas, meteoric ^{10}Be rains down onto the land and ocean surfaces, where it is adsorbed to the outside of particles or incorporated into secondary phases such as Mn and Fe-oxides where it mixes with ^{9}Be sourced from weathering of the primary minerals (Willenbring and von Blanckenburg, 2010). The relatively constant flux of ^{10}Be to the earth's surface at any one location over time means that ^{10}Be/^{9}Be ratios and ^{10}Be concentrations provide useful measures of soil formation (e.g. Pavich et al., 1984), sediment transport pathways and provenance in riverine environments (Brown, 1987). In the marine environment meteoric ^{10}Be is efficiently and quickly transported from surface waters via biological pathways to the sea bed (Frank et al., 1997), a property which has been used to monitor weathering and sequestration of CO_2 on glacial/interglacial cycles (e.g. von Blanckenburg et al., 2015).

Ice sheets transport and disperse beryllium isotopes in a way that differs markedly to that in temperate or tropical systems. The sources and transport pathways of ^{9}Be and ^{10}Be across the major ice outlets of continental scale ice sheets are largely separated (Graly et al., 2018). ^{9}Be is sourced primarily by glacial erosion and is transported in sediments that are concentrated in the basal zone (lower few meters and the deforming bed; Fig. 1). Meteoric ^{10}Be produced in the atmosphere is deposited with snow and then found throughout the ice column (Beer et al., 1987), which is largely debris-free. During seaward transport by the ice sheet there is limited or no mixing of these two components, unlike riverine systems where mixing occurs both at the source and dur-

* Corresponding author.
E-mail address: duanne.white@canberra.edu.au (D.A. White).

https://doi.org/10.1016/j.epsl.2018.10.004

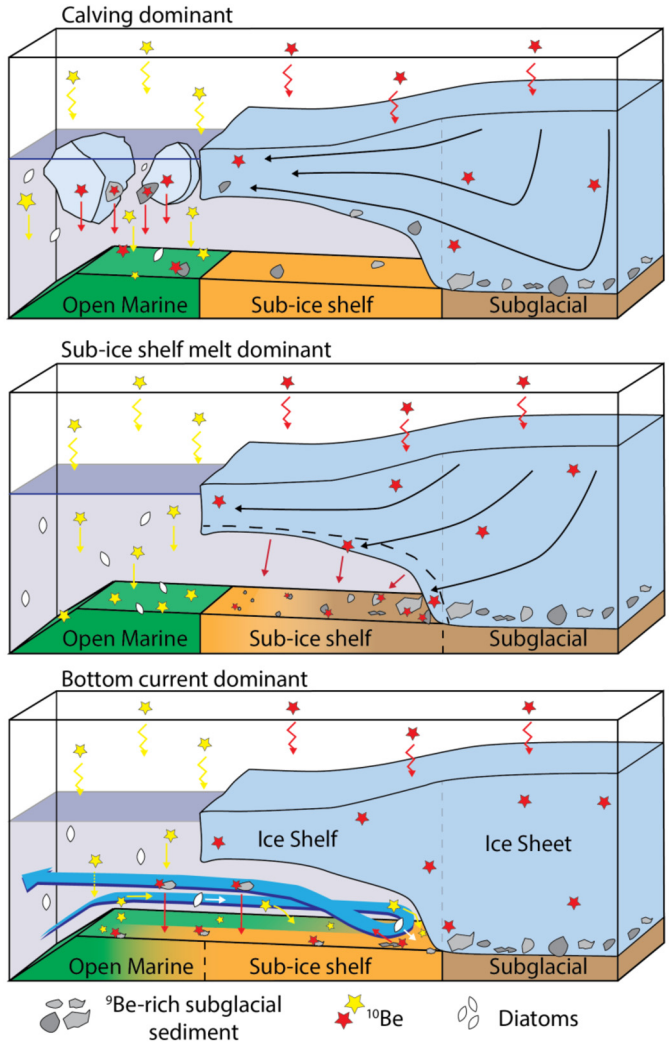

Fig. 1. Conceptual models of the influence of different glacial and marine processes on the distribution of Be isotopes in marginal marine and ice-shelf environments. Top (after Yokoyama et al., 2016); if iceberg calving is the dominant process of ice loss, any continental sediment released underneath ice shelves will have very low ^{10}Be concentrations, as all terrestrially sourced ^{10}Be is transported seaward into the open marine environment. Middle; if sub-ice shelf melt is active (dotted line), ^{10}Be from melting ice will be deposited in sediments in the sub-ice shelf cavity, although the high sediment generation rates near the grounding line causes ^{10}Be concentrations to be lower than in the open marine settings, especially close to the ice sheet. Bottom; if strong bottom currents are active, sediments from open marine environments high in ^{10}Be, organic matter and diatoms are transported into the sub-ice shelf cavity, reworking and mixing ^{10}Be concentrations and ^{10}Be/^{9}Be ratios in sediment throughout the marine portion of the system.

ing transport. Thus, ice sheets can deliver their isotopic beryllium fluxes from continental interiors to coastal margins in a spatially segregated manner, with limited interaction during transport. This means there is little opportunity for sediments entrained in the ice to mix their Be isotope fluxes and set a locally representative ^{10}Be/^{9}Be ratio. The independent pathways in Be isotopes in glacial environments results in generally low-meteoric ^{10}Be concentrations in sediments produced by glacial transport, which has successfully been applied as a marker for presence and absence of ice sheets (Scherer et al., 1998).

There have been relatively few studies to determine how different modes of beryllium transport in ice affects their distribution on glaciated continental and marine margins. Existing studies from the Ross Sea sector of Antarctica (Sjunneskog et al., 2007) suggest a strong positive ^{10}Be concentration gradient between the ice sheet and the continental shelf. There are indications that sub-ice shelf sediments, traditionally challenging to identify in sediment cores using existing proxies (Post et al., 2014), may be recognised from their relatively low ^{10}Be concentrations (Yokoyama et al., 2016). However, the utility of ^{10}Be as an ice shelf proxy relies on calving of icebergs at the ice shelf front transporting meteoric ^{10}Be deposited on the ice shelf and sheet to the open marine environment, thus preventing ^{10}Be reaching sub-ice shelf sediments in the ocean cavity (Fig. 1, top). Other marine-margin processes such as basal ice-shelf melt and sub-ice shelf ocean circulation may also influence spatial distribution of Be isotopes (Fig. 1, middle and bottom), but the rate and role of these processes is poorly quantified. The influence of sub-ice shelf processes may limit our ability to correlate Be isotopes in sediment to the dynamics of ice sheet retreat and advance, and understand the effect of glacial–interglacial cycles on beryllium cycling in the global ocean. Thus, more information is required to better understand the depositional environments and processes which control Be isotope concentrations.

In this paper we investigate the distribution of beryllium isotopes and their range in concentration in sediment from Prydz Bay, the outlet for the Lambert Glacier–Amery Ice Shelf system. This area presents a useful case study, as the processes of oceanic circulation (Galton-Fenzi et al., 2012), sediment transport (Post et al., 2014), and ice shelf (Hemer and Harris, 2003) and ice sheet history (e.g. Domack et al., 1998; White et al., 2011) in this sector of the Antarctic coastal margin are relatively well defined. It is also an area where strong oceanic circulations on the continental shelf and in the sub-ice shelf cavity blur the physical and biological characteristics of different glacio-marine environments (Hemer et al., 2007; Post et al., 2014) and thus pose challenges to traditional sedimentological models of proximal glacio-marine sedimentation (e.g. Domack and Harris, 1998) used to identify past ice shelf extents.

Here, we aim to distinguish how sub-ice shelf circulation affects the Be isotopic composition of sediments in differing environmental settings and relate these to oceanic and glacial environments and processes. We investigate whether Be isotopes can be generally applied as a tracer of different depositional settings along a transect from a continental ice sheet, to the grounding line zone (where grounded ice begins to float and interact with the ocean) along the sub-ice shelf setting to an open marine continental shelf environment.

2. Environmental setting

At the northern extension of the Lambert Glacier–Amery Ice Shelf System, the Amery Ice Shelf is the drainage point of eight tributary glacial basins the largest of which are the Lambert and Mellor Basins (Fig. 2). The system drains 16% of the East Antarctic Ice Sheet, transmitting 88.2 ± 2.9 Gt a year, making it a significant contributor to the overall ice mass balance of Antarctica (Yu et al., 2010; Post et al., 2014).

The Amery Ice Shelf is approximately 450 km long and thins from a maximum of over 2500 m at the southern grounding line to around 200 m at the shelf front. The thickness of the sub-ice cavity ranges from 250 m to 1600 m (Galton-Fenzi et al., 2008), with a high basal melt rate compared to other East Antarctic ice shelves (Pritchard et al., 2012).

The Lambert–Amery system drains into Prydz Bay, where steep bathymetry and topography allows for currents to form the strong clockwise circulation of the Prydz Bay Gyre. Modified Circumpolar Deep Water flows from the east over Four Ladies Bank, where it intersects the East Wind Drift current, carrying fresh ice shelf water from West Ice Shelf and highly saline water produced in the sea-ice free area of the Barrier Polynya (Williams et al., 2016). Here, the current splits, with part continuing westward across the

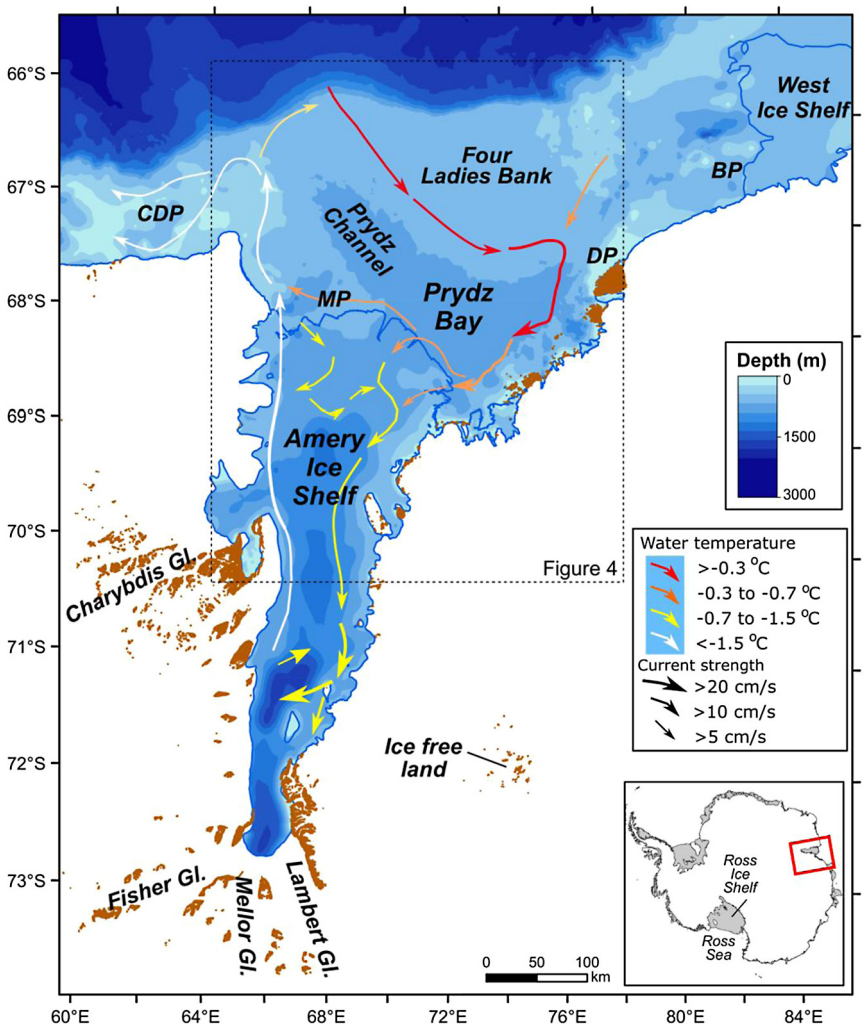

Fig. 2. Map of Lambert Glacier–Amery Basin, Prydz Bay, modern ice shelf edge (blue line) and location of current grounding line. Sites discussed in the text, showing location of key ice shelves, open marine and sub-ice shelf bottom currents. Note the strong gyre-like circulation underneath Amery Ice Shelf (after Galton-Fenzi et al., 2012), and the differing characteristics of water masses in Prydz Bay, and the eastern and western sides of the sub-ice shelf cavity. CDP, MP, DP and BP indicate Cape Darnley, Mackenzie, Davis and Barrier Polynyas respectively. Red box in inset on lower right indicates location of main map. Sea-bed elevation (metres below sea level) from IBSCO compilation shown for areas seaward of the grounding line. (For interpretation of the colours in the figure(s), the reader is referred to the web version of this article.)

ice shelf front, while the remainder flows south into the sub-ice shelf cavity of the Amery Ice Shelf (Fig. 2). Below the Amery Ice Shelf, these two currents mix and form a highly saline water mass, which then sinks. The back-sloping bathymetry of the Amery Ice Shelf cavity and Coriolis effect drives these currents along an eastern channel below the Amery Ice Shelf towards the grounding line, causing significant basal melt. Here, the now fresher melt water rises and follows the clockwise gyre along the western margin of the Amery Ice Shelf, and is ejected into Prydz Bay as Ice Shelf Water, completing the 'ice pump' driven circulation typical of Antarctic sub-shelf circulation systems (i.e. Herraiz-Borreguero et al., 2015). Ice Shelf Water from the Amery Ice Shelf is mostly recirculated through the Prydz Bay Gyre back under the ice-shelf, but some flows westwards out of the bay (Fig. 2).

In the open marine environment, in particular on the western flank of the Prydz Channel depression, currents can exceed 1 cm/s (Nunes Vaz and Lennon, 1996). Flow speeds can be even greater under the Amery Ice Shelf, which has a strong sub-ice shelf current system (∼5–10 cm/s; Fig. 2). Sub-ice shelf currents under the Amery are substantially more vigorous than other large ice shelves (e.g. Ross Ice Shelf, 1 cm/s; Jenkins et al., 2003; Post et al., 2014), and is capable of depositing sediment from a marine environment great distances beyond the ice front.

3. Methods

The Prydz Bay region has been the focus of several decades of geophysical mapping and sediment coring. Sediment grabs, gravity and piston cores have been collected on cruises by the *Aurora Australis* (186 & 901), Joides Resolution (Leg 188, 2000), Nathaniel B. Palmer (NBP01, 2001) and Polarstern (XXIIV, 2007). Cores have also been collected from underneath the Amery Ice Shelf through the AMISOR program (Allison, 2003). For this paper, we investigated material from *Aurora Australis* cruises 186, 901 and the AMISOR program, which has been preserved at 4 °C since collection.

To investigate the modern distribution of ^{10}Be in Prydz Bay sediments, we selected samples from core top (surficial) sediments representative of different modern depositional environments. Seven core-top samples from open marine (labelled as GC) and six sea-bed samples from sub-ice shelf (labelled as AM01–06) environments were obtained from a wide geographic area (Table 1). Open marine sediment samples were restricted to areas where iceberg turbation is absent, or in the case of GC18, potentially limited. Core top GC27 was sampled by ship in open marine conditions adjacent to the ice shelf margin but is now covered by the ice shelf. Observations of the shelf-front position since

Table 1
Beryllium isotope and core location data.

Core name	Cruise	Water depth[a] (m)	Core depth[b] (cm)	Latitude	Longitude	Sample mass (g)	^{9}Be total[c] (μg/g)	^{9}Be HCl extracted (μg/g)	^{10}Be HCl extract[d] (10^6 at/g)	^{10}Be/9 HCl ext. (10^{-8} at/at)
Open marine core tops										
GC22	901	766	0	68.065	72.2760	0.41	–	0.22	785.1 ± 18.4	5.5
GC27	901	776	0	68.947	73.5858	0.68	–	0.25	985.6 ± 22.7	5.8
GC29	901	789	4	68.663	76.6955	0.34	–	0.18	847.1 ± 19.8	7.1
GC24	901	705	0	68.094	73.1893	0.46	–	0.21	892.1 ± 20.7	6.2
GC15	186	1050	1	68.518	70.4075	0.86	–	0.12	173.2 ± 4.5	2.2
GC16	186	726	4	68.375	71.3070	0.70	–	0.13	347.7 ± 10.4	4.1
Sub-ice shelf core tops										
AM01B	AMISOR	840	0	69.431	71.4462	0.62	2.01	0.49	810 ± 19.6	2.5
AM02	AMISOR	843	0	69.713	72.6400	0.44	–	0.64	1110 ± 28.7	2.6
AM03	AMISOR	1339	0	70.561	70.3322	1.35	2.58	0.53	838.3 ± 19.2	2.4
AM04	AMISOR	1002	0	69.900	70.2903	1.36	2.61	0.50	457.5 ± 10.5	1.4
AM05	AMISOR	979	1	70.230	69.6967	1.79	2.73	0.44	248.3 ± 5.7	0.8
AM06	AMISOR	902	0	70.250	71.3500	2.11	2.41	0.27	508 ± 11.8	2.8
Basal diamicts (subglacial)										
AM01b	AMISOR	840	45	69.431	71.4462	2.75	–	0.32	31.1 ± 1.1	0.1
AM04	AMISOR	1002	115	69.900	70.2903	2.51	–	0.24	36.2 ± 0.9	0.2
GC16	186	726	227	68.375	71.3070	2.13	–	0.42	160.9 ± 4.1	0.6
GC24	901	705	431	68.094	73.1893	2.32	–	0.42	86.3 ± 2.2	0.3
GC29	901	789	351	68.663	76.6955	2.27	–	0.17	100.7 ± 2.4	0.9
Shallow water										
GC18	901	320	1	67.283	76.5703	0.71	–	0.35	776 ± 18.2	3.3
Down-core										
AM01b[*]	*AMISOR*	*840*	*0*	*69.431*	*71.4462*	*0.62*	*2.01*	*0.49*	*810 ± 19.6*	*2.5*
AM01b	AMISOR	840	4	69.431	71.4462	0.77	–	0.45	766.1 ± 17.9	2.5
AM01b	AMISOR	840	11	69.431	71.4462	1.13	2.22	0.48	813.8 ± 18.7	2.5
GC22[*]	*901*	*766*	*0*	*68.065*	*72.2760*	*0.41*	–	*0.22*	*785.1 ± 18.4*	*5.5*
GC22	901	766	13	68.065	72.2760	0.57	–	0.29	757.6 ± 18.3	3.9
GC22	901	766	22	68.065	72.2760	0.57	–	0.54	703.8 ± 16.4	2.0
Repeat analyses										
GC24-1[e]	901	705	0	68.094	73.1893	0.39	–	0.24	834.8 ± 19.7	5.1
GC24-1b[f]	901	705	0	68.094	73.1893	N/A	–	–	47.1 ± 1.4	
AM05-2[e]	AMISOR	979	1	70.230	69.6967	1.34	2.73	0.45	252.4 ± 6	0.8
AM05-2b[f]	AMISOR	979	1	70.230	69.6967	N/A	2.73	–	14.5 ± 0.5	

[a] Water depth for open marine cores, depth below grounded ice shelf surface for sub-ice shelf cores.
[b] Sediment sub-sample depth below core top.
[c] Total ^{9}Be content from complete HF dissolution of dry sediment aliquot.
[d] ^{10}Be uncertainties are 1σ standard errors.
[e] Repeat from a second sediment aliquot and full processing.
[f] Repeat leaching of leached sediment used in first GC24-1 and AM05-1.
[*] Duplicated data entries (in italics) from the marine and sub-ice shelf core tops for ease of capturing the down core trends.

1936 suggests this site is likely open marine for at least 80% of the 60–70 yr calving cycle (Fricker et al., 2002). Core top sediments from open marine and sub-ice shelf environments are all fine grained, with varying siliceous content in open marine environments of 1 to 50%, and of diatom abundance in sub-ice shelf sediments of 0 to 160 × 10^6 valves/g (Post et al., 2014).

The nature of gravity coring means the surficial sediments may have been disturbed or not retained, and thus there is some potential our samples may not represent the most recently deposited sediment. Available radiocarbon dating (e.g. Post et al., 2014) and comparison with ages of known surface samples (Domack et al., 1991) indicates that if this has occurred, our sediments are latest Holocene in age, likely the last ∼1 ka. To understand the temporal variations that may have influenced the Be isotope concentrations, we supplemented the core top sediments with a limited number of down-core samples. Holocene siliceous marine ooze (SMO) from open marine (GC22, depths of 13 and 22 cm) and sub-ice shelf (AMO1B, 4 and 11 cm, Table 1). The limited variation present in Be isotope concentration across Holocene timescales provides confidence that the difference in ^{10}Be concentrations in our core tops across the region reflect geographic rather than temporal variations.

Depth samples were also taken from basal sands and diamict facies interpreted as grounding line or subglacial sediments from a range of sub-ice shelf and open marine cores (AMO1B [depth 45 cm], AMO4 [115 cm], GC16 [227 cm], GC24 [431 cm] and GC29 [351 cm]).

We used a HCl extractant chemistry process to release both ^{9}Be and ^{10}Be from the sediments (Knudsen et al., 2008). This approach effectively removes the full authigenic meteoric ^{10}Be fraction without accessing *in-situ* ^{10}Be. Sediment was collected from 1 cm thick sections, dried overnight at 100 °C, and then reacted with 10 ml of 6 M HCl for 3 h at room temperature. The solutions were then split into two aliquots to separately measure concentrations of ^{9}Be by ICP-OES and ICP-MS at the University of Canberra and cosmogenic ^{10}Be by Accelerator Mass Spectroscopy. The aliquot removed for ^{9}Be was ∼ 20% of total extracted solution and was sufficient to achieve a repeatability of <5% for ^{9}Be assays in the range 100 to 500 ppb.

For the AMS analysis, the second aliquot was spiked with 0.22 or 0.45 mg of ^{9}Be prepared from beryl crystal with a negligible ^{10}Be content. Beryllium was isolated from the solutions using methods described in Child et al. (2000), oxidised, mixed with Nb powder and pressed into AMS targets (Fink et al., 2000). Fi-

nal $^{10}Be/^{9}Be$ ratios were corrected by full chemistry procedural blanks and normalized to the NIST-4325 $^{10}Be/^{9}Be$ AMS standard using a nominal ratio of 27,900 $\times$ 10^{-15} (Fink and Smith, 2007; Nishiizumi et al., 2007). Full procedural blanks gave a mean $^{10}Be/^{9}Be$ ratio of 20 $\pm$ 10 $\times$ 10^{-15} ($n = 2$), which was equivalent to 0.5% the ratio measured for the lowest sediment sample. Final analytical error in concentrations (atoms/gram) were derived from a quadrature sum of the larger of the total statistical error or standard mean error from repeat AMS ratios (typically 1%), 2% for AMS standard reproducibility and 1% in Be spike.

To assess that our chemistry methods were reproducible with respect to equivalent extraction efficiencies, full replicate procedural measurements were carried out on two core-top samples (GC24, AM05) starting from unprocessed sediment sub-samples resulting in ^{10}Be concentrations consistent within 1 and 5% respectively. While 6 M HCl has been shown to quantitatively extract the meteoric ^{10}Be component in marine sediment (Knudsen et al., 2008), we further tested the quantitative nature of the HCl extraction by conducting a second 6 M HCl leach on the same leached sediment aliquots of GC24-1 and AMO5-1 used above. The second repeat leach extracted a further ~1–3% of the ^{10}Be extracted in the first leach. A similar result was given for whole-sediment concentrations of most major elements, although this was higher for the more refractory elements, suggesting most of the more mobile fractions of the sediment had been dissolved by the first leach. These tests suggest that the HCl extraction is sufficiently aggressive to quantitatively remove the meteoric (mobile) component of the sediment.

To assess that fraction of element concentrations leached via our chemistry procedures to their total whole sediment concentration, regardless of affinity, we compared extracted solutions to assays in HF-based total digest (Bourles et al., 1989). Between 10 and 30% (mean of 23%) of the total Be present in the sediment was extracted by the 6 M HCl leach on fresh sediment, values similar to that obtained via weaker extraction techniques used to target 'reactive' ^{9}Be in Antarctic sediments (Valletta et al., 2018). There were no obvious trends between Be extraction efficiency and sample characteristics such as mineralogy or total Be concentration. The first HCl leach typically extracted ~30% of the more soluble major elements (Fe, Mn, Na, K), and 10% of more refractory elements (Ti, Al), consistent with existing studies (e.g. Larner et al., 2007) indicating it is capable of extracting the adsorbed, oxide, carbonate and organic fractions of the sediment.

Lastly, we compared our beryllium isotope measurements to a range of sediment characteristics to better understand the processes that influence isotope concentrations and ratios. Data was sourced from available core-top analyses of grainsize, diatom abundance, opal and percent modern radiocarbon (from core-top bulk organic radiocarbon ages) previously analysed from Prydz Bay (O'Brien et al., 1995; Harris et al., 1998; Taylor and Leventer, 2003) and under the ice shelf (Post et al., 2014). Holocene sedimentation rates at each site were estimated based on radiocarbon dating where available (Domack et al., 1998; Taylor and McMinn, 2002; Post et al., 2014), or the assumption that biogenic sedimentation began shortly after ice decoupled from the bed across the region around the beginning of the Holocene (Domack et al., 1998; Hemer and Harris, 2003).

4. Results

In the Prydz Bay region, we observed distinct differences in ^{10}Be and ^{9}Be concentrations of sediments deposited in the three major ice-marginal depositional environments (open marine, sub-ice shelf and inferred subglacial/grounding line; Fig. 3, Table 1). Be-isotope concentrations and ratios were generally within the range of those reported elsewhere on the Antarctic continental shelf and slope (Frank et al., 1995; Sjunneskog et al., 2007; Valletta et al., 2018). However, the relationship between environment and Be isotope concentrations was substantively more complex than previously reported from the continental shelf (Sjunneskog et al., 2007), with isotope concentrations varying by up to a factor of five within each environment. Apart from lower ^{10}Be concentrations in subglacial environments, no single concentration provided a unique signature of depositional environment. Spatial trends in the beryllium isotope concentrations in Prydz Bay provide insight into the different sources and processes that influence ^{10}Be and ^{9}Be concentrations in ice marginal marine sediments.

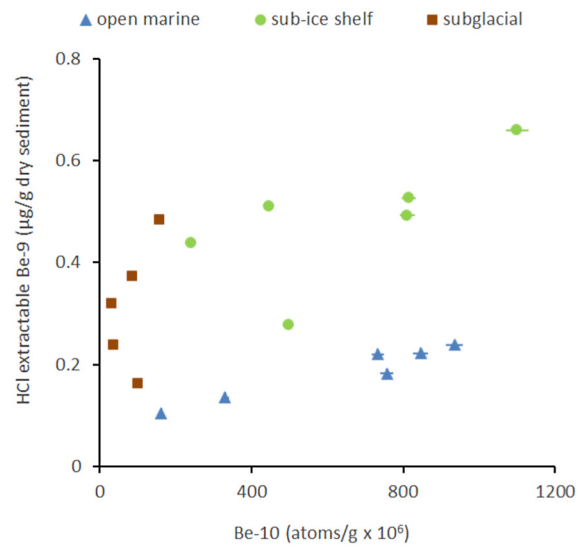

Fig. 3. ^{10}Be vs HCl extractable ^{9}Be in Prydz Bay. Open marine and sub-ice shelf are core-top sediments in their respective environments in Prydz Bay and under the Amery Ice Shelf, while 'subglacial' sediments are basal diamicts in selected cores both under the ice shelf and in Prydz Bay. Note that both isotopes are needed to discriminate samples from the three environments, though all sub glacial sediments can largely be differentiated by ^{10}Be alone. Error bars represent 1σ standard errors.

4.1. ^{10}Be

Modern, core-top ^{10}Be concentrations in open marine (~200–1000 $\times$ 10^6 at/g) and sub-ice shelf environments (250–1100 $\times$ 10^6 at/g) displayed substantial variation within, and overlap between, the two geographically different depositional environments. Biogenic poor, basal diamicts inferred to have been deposited in subglacial settings (30–160 $\times$ 10^6 at/g) were distinctly lower than modern (core top) sediments.

The spatial variation in core-top ^{10}Be concentrations follows the pattern of open marine and sub-ice shelf circulation. Higher values are present in the central and eastern parts of Prydz Bay, and the 'inflow' sector underneath the ice shelf. Much lower values are present on the western, 'outflow' side of the ice shelf, and the open marine immediately north of the calving margin of the ice shelf, where sub-ice shelf water discharges into Prydz Bay (Fig. 4).

Variation over Holocene times (i.e. down-core) within the SMO horizons was limited, confirming the environmental conditions during this period were broadly stable (Table 1). This confirms that core-top sediments provide an accurate representation of modern depositional processes for both open marine (GC22) and sub-ice shelf settings (AM01B).

4.2. ^{9}Be

In contrast, HCl extractable ^{9}Be variability is more subdued, with intra and inter-group variability halved that seen in ^{10}Be. HCl extractable ^{9}Be was generally higher underneath the ice shelf

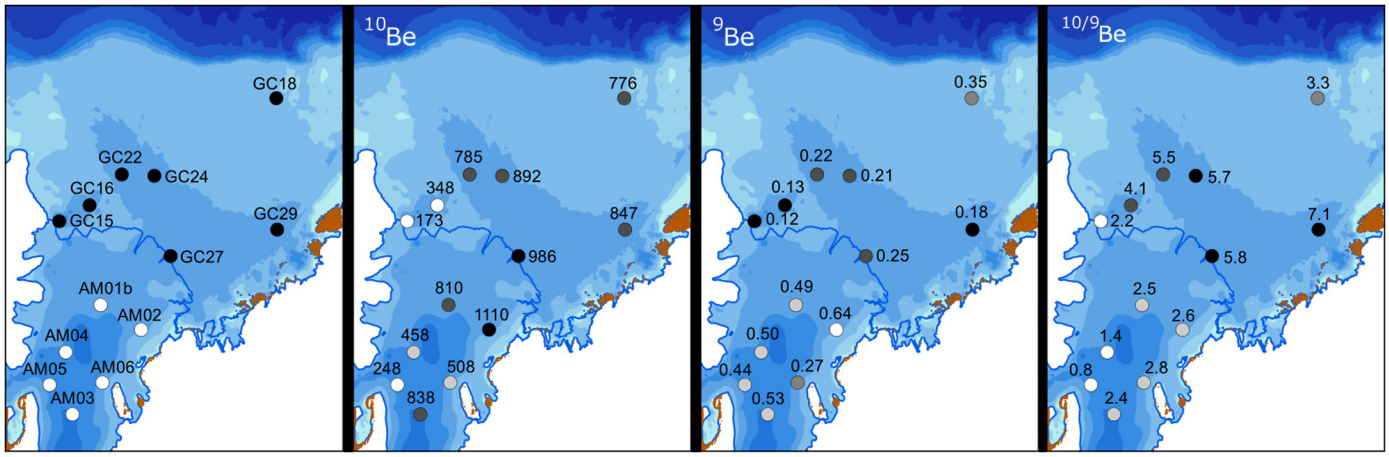

Fig. 4. Core locations (left) and core-top results for HCl extractable ^{10}Be (10^6 at/g), ^{9}Be (µg/g) and ^{10}Be/^{9}Be ratio (10^{-7} at/at) concentrations. In each plot, the samples dominated by a terrestrial sediment source of Be isotope concentrations or ratios are shown as white dots, and sediments dominated by an open ocean source of Be isotopes are shown as black dots, with a 3 level grey-scale for values between the two limits. Note that the ice shelf has expanded over core site GC27 since collection, as part of a 60–70 yr calving cycle (Fricker et al., 2002).

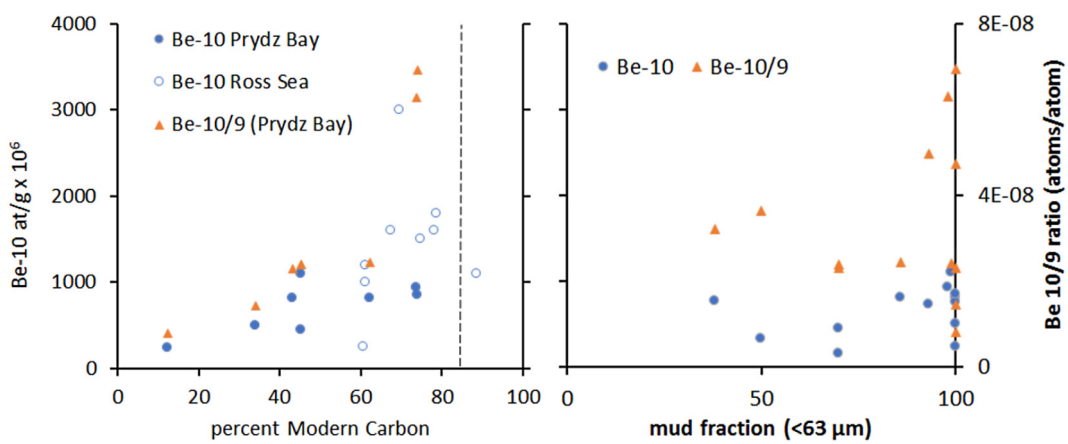

Fig. 5. Relationship between percent Modern Carbon and ^{10}Be concentration (left panel; Ross Sea, Sjunneskog et al., 2007; Yokoyama et al., 2016 and Prydz Bay), and <63 µm mud fraction to Be isotopes values (right panel; Prydz Bay) from core top (i.e. modern) sediments. Vertical dotted line in left hand panel represents the percent Modern Carbon (pMC) of pre-bomb waters and typical carbonate shells on the Antarctic continental shelf (Berkman and Forman, 1996), including under the modern Amery Ice Shelf (Post et al., 2014).

(range = 0.27–0.64 µg/g) than in open marine (0.12–0.25 µg/g), with subglacial sediments showing intermediate values (0.17–0.42 µg/g, Fig. 3).

4.3. ^{10}Be/^{9}Be ratios

The ^{10}Be/^{9}Be ratio in the HCl extractable portion of the sediment provided improved discrimination between the three depositional environments than either of these values alone. The ratio also allowed discrimination of additional geographic trends that were not observable in the raw concentrations.

The lowest ^{10}Be/^{9}Be ratios were observed in subglacial sediments (0.1–0.9 × 10^{-8} atoms/atom), while the highest values were found in the open marine environment of east Prydz Bay (5–7 × 10^{-8}). Sediment in the eastern, inflow side of the ice shelf produced a narrow range of ^{10}Be/^{9}Be ratios (2.5–2.8 × 10^{-8}), despite wide variation in the raw concentrations of both. Sediment on the western, outflow side of ice shelf cavity (<1 × 10^{-8}) and in open marine environments immediately north of calving margin on the outflow (2.2–4.1 × 10^{-8}) provided lower values than their equivalents in the eastern/inflowing side of the circulation.

4.4. Comparison to other sediment components

Our sampling was biased toward the mud-rich surface sediments, namely siliceous muddy ooze. However, within the geographic range that we have covered, there is little observed correlation between grainsize and either ^{10}Be concentrations or ^{10}Be/^{9}Be ratios. HCl extractable ^{10}Be and ^{9}Be are poorly correlated with abundance of the mud fraction ($R^2 = 0.1$ and 0.3 respectively, Fig. 5). In addition, in all three measures (^{9}Be, ^{10}Be, and the ^{10}Be/^{9}Be ratio), samples with 100% mud fraction exhibit the full range of values observed in the dataset. The limited correlation between Be isotope values and the sediment grainsize, suggests that although some partitioning may be present (e.g. Wittman et al., 2012), the delivery and deposition of Be isotopes in sub-ice shelf and open marine environments in this sector of the Antarctic continental shelf are not controlled primarily by grainsize. In turn this implies that the Be isotopes extracted from bulk sediment (i.e. the HCl extractable or 'reactive' Be) via our HCl leaching process were well equilibrated within the water column prior to being incorporated in the authigenic phase of the sediment. Similarly, the absence of correlation (R^2 of 0.1 or less) between sedimentation rate and either of the Be isotope concentrations indicates that

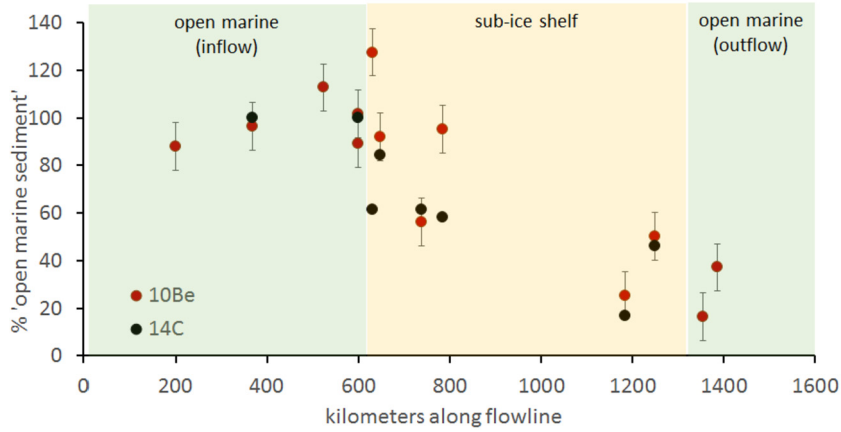

Fig. 6. Sediment advection and mixing along a bottom current flowline as inferred from a two-component mixing model using both ^{10}Be and ^{14}C as proxies for sediment source. Flowline distance follows the trajectory of bottom currents in Fig. 2, starting from off the continental shelf, moving clockwise to the southern grounding line under the ice shelf, and then returning north along the western boundary of the ice shelf. The overall reduction in the open marine sediment fraction along the flowline moving from inflow to outflow zones (i.e. with increasing distance underneath the shelf) suggests ^{14}C and ^{10}Be concentrations are primarily controlled by sediment advection, and an increasing admixture of continental sediment. Secondary processes (such as vertical mixing, storage, cross current flows) may explain the offset from a simple two-member linear mixing model.

core-site sedimentation rates are not the primary control on local ^{9}Be or ^{10}Be concentrations.

The correlation between the ^{10}Be concentrations was explored against several measures of the biogenic component of the sediment, including diatom abundance, opal and radiocarbon reservoir ages. Diatom varve counts are available for most sub-ice shelf (Post et al., 2014) and a few open marine sites (Taylor and Leventer, 2003), while measurements of biogenic opal are only available for open marine sediments (O'Brien et al., 1995; Harris et al., 1998). Both measures (diatom count and biogenic opal) correlate only weakly with both ^{10}Be concentration ($R^2 = 0.2$) and ^{10}Be/^{9}Be ratios ($R^2 = 0.3$). Beryllium concentrations and ratios are much more strongly correlated with the radiocarbon 'age', perhaps best expressed by the linear correlation between percent Modern Carbon (pMC; defined as the measured sample radiocarbon normalised to atmospheric radiocarbon content at 1950 referenced to the Oxalic acid-II standard) and ^{10}Be concentrations ($R^2 = 0.5$) and ^{10}Be/^{9}Be ratios ($R^2 = 0.8$; Fig. 5).

Tellingly, the linear trend between ^{10}Be concentration and pMC in surface sediments intersects the origin (Fig. 5). This result would be expected if ^{10}Be concentrations are a product of two component mixing, with end members being dominated by terrigenous sediments (low/near zero ^{10}Be and pMC) and biogenic marine sediments (high ^{10}Be and pMC) respectively. Within the sub-ice shelf cavity, both the ^{10}Be concentrations and pMC decrease along the flow-path of sub-ice shelf circulation (Fig. 1, Post et al., 2014), with the lowest values of both found at AM05 on the outflow side of the cavity.

5. Discussion

5.1. What determines sediment ^{10}Be concentrations in Antarctic shelf environments?

The high ^{10}Be concentrations from underneath Amery Ice Shelf (AM0 1–6 cores tops) which overlap with open marine values are incompatible with a 'calving dominant' process of ^{10}Be distribution as shown in Fig. 1(top). This contrasts with that observed by Yokoyama et al. (2016) in a study of Ross Ice Shelf retreat. Here, we consider that all three processes depicted in Fig. 1 – calving, subglacial melt, and strong bottom (sub-surface cavity) currents may all have a role in influencing ^{10}Be concentrations in the Prydz Bay sub-ice shelf region.

To aid interpretation of the ^{10}Be distribution, we use a two end-member mixing model, where sediment is derived from two primary sources: (1) open marine settings and (2) continental sources derived from ice eroding bedrock and older sediments. The proportion of sediment mixing is estimated using end-member source values for ^{10}Be and ^{14}C as proxies along the clockwise current gyre commencing at the continental shelf break to the southern grounding line, returning northwards to the shelf break for a total distance of about 1400 km. The model successfully captures the first-order mixing behaviour of the two isotopes seen in the raw data of Fig. 6, suggesting a two-component mixing is the primary control on the ^{14}C and ^{10}Be concentrations in the sediments. However, given the potential complexity in the system we also identify instances where other factors may have influenced concentrations of these isotopes in sediments in Prydz Bay.

Sediment originating from the open marine environment is primarily biogenic, with the potential for a mineral component derived from ice rafted debris and dust. ^{10}Be concentrations in these environments are a function of the ^{10}Be deposition rate (derived from direct atmospheric deposition and ice melt) and the sediment mass flux. The maximum core top ^{10}Be concentrations in open marine settings in Prydz Bay (~800–1000 $\times$ 10^6 at/g) are like those deposited in the modern open ocean (von Blanckenburg et al., 2015). However, the average concentration in Prydz Bay sediments are lower than those observed in the Ross sea (Sjunneskog et al., 2007) (Fig. 5). Thus, the true ^{10}Be concentration of recently produced biogenic sediment in Prydz Bay may be partially masked by bottom currents redepositing reworked sediment from the continental shelf with lower ^{10}Be concentrations. However, the similarity in the core-top sediments across eastern Prydz Bay suggests that if this is the case, the sediments presently being deposited on the continental shelf are relatively well mixed, either in the water column or by post-depositional reworking by bottom currents. Based on this interpretation, we assign the end member values in our mixing model for open marine sediments of 74% modern for ^{14}C and 877 $\times$ 10^6 at/g for ^{10}Be, calculated as the average of core top-sediments from Prydz Channel (GC 22–27).

Sediment derived from primary continental sources is assumed to be dominantly lithogenic, sourced by glacial erosion of pre-Cenozoic (and largely Precambrian) bedrock that lies underneath most of the modern Lambert Glacier–Amery Ice Shelf drainage system (Mikhalsky et al., 2001). The subglacially derived sediment is expected to have very low ^{10}Be concentrations, reflecting the lithogenic sources, although subglacial melt of meteoric ice

may contribute some ^{10}Be to the sediment (Graly et al., 2018). These source sediments are also expected to have a biogenic component derived from Cenozoic and Mesozoic sediments present underneath the modern outlet glaciers (e.g. Mishra et al., 1999; White et al., 2011), which would include an organic carbon fraction with effectively zero pMC. Sub-glacial basal diamicts sampled from the Prydz Bay continental shelf have ^{10}Be concentrations of $\sim 100 \times 10^6$ at/g (Table 1, GC cores) with little spatial variation or temporal variation during former glacial advances across Prydz Channel (Guitard, 2015). Concentrations from the basal diamicts further south underneath the Amery Ice Shelf ($\sim 30 \times 10^6$; Table 1, AM0 cores) are lower than in Prydz Bay, likely reflective of an increased continental component, which dilutes the open marine signal or alternatively a reduced input of reworked open marine material. None of the subglacial sediments we measure from beneath the Amery Ice Shelf have ^{10}Be concentrations that are as low as those measured in modern subglacial settings ($\sim 8 \times 10^6$ atoms/g, Sjunneskog et al., 2007), suggesting that we may not have sampled this primary source. For our continental end member in our mixing model, we utilize the basal diamicts from under the ice shelf (AM01 & 4, ^{10}Be of 34×10^6 at/g, assumed radiocarbon dead).

We interpret ^{10}Be and ^{14}C concentrations at our sampling locations along the clockwise bottom current flow-line that fall between these two component sources (i.e. subglacial lithogenic, 34×10^6 at/g, and zero pMC with open marine 877×10^6 atoms/g and 74% pMC) to be primarily the result of a two-source sediment mixing process (see Fig. 6). Mixing could occur either by (horizontal) mixing of primary sources in the modern-day environment via ocean circulation, or by (vertical) mixing of sediment by glacial deformation of underlying, and thus chronologically differing horizons.

Both the ^{10}Be and ^{14}C concentrations in core tops under and near the modern ice shelf provide evidence for horizontal mixing of the two primary sediment sources on length scales of several hundred kilometres (Fig. 6). Some of our sub-ice shelf sites on the eastern, inflow side of the shelf (AM01, 2 and 3) have ^{10}Be concentrations identical to those deposited in modern open marine environments in Prydz Bay (GC24, 27 and 29), and thus are inferred to have sourced almost all their sediment from advection from the open marine environment. These high concentrations are primarily toward the front of the ice shelf, but also in the central portion (AM03) where modelled sub-ice shelf circulation is directly from Prydz Bay (Galton-Fenzi et al., 2012) with little interaction with the ice shelf margins. Other proxies in these sites such as diatom concentrations (Post et al., 2014) indicate that sediments deposited at AM01, 2 and 3 are also compatible with a wholly open marine component of the sediment.

Mixing-model values using the radiocarbon concentrations suggest a lower open marine component in some of the sub-ice shelf core-tops than ^{10}Be (AM01 & 3, Fig. 6), which may be a function of either differential transport pathways for ^{10}Be and ^{14}C, or some reworking of late Quaternary open marine sediment from which ^{14}C has decayed.

Further support for the bottom current advection model is provided by the ^{10}Be and ^{14}C concentrations at AM05, which sits on a modelled outflow zone ($\sim$1200 km along the mixing line). While concentrations are low ($\sim 250 \times 10^6$ at/g), they never reach the very low concentrations seen in modern subglacial conditions in west Antarctic outlet glaciers (Sjunneskog et al., 2007). There are two possibilities for the lack of a dominant continental ^{10}Be signature in the sub-ice shelf sediments at this location; (1) advection of sediment from the open marine setting extends as far south as $\sim$ 200 km from the modern ice shelf edge against the outflow zone, so none of our sites are truly dominated by subglacial sediment (2) ^{10}Be is released from melt of the base of the ice shelf, and attaches to continental-derived sediment delivered at the grounding line and moved by outflow cavity currents in quantities sufficient to provide a 'mixed' ^{10}Be signal (i.e. the sub-ice shelf melt process of Fig. 1). We consider there is supporting evidence for both processes. AM05 has little to no diatom abundance, suggesting limited advective transport of clay or silt sized particles from open marine settings, which would mean the ^{10}Be at this site is derived from local sources (i.e. sub-ice shelf melt). However, radiocarbon concentrations at this site imply a small fraction of the organic component of the sediment ($\sim$10%) is derived from modern sources, supporting advection (Post et al., 2014). In either case, the measured ^{10}Be concentrations in the range of $\sim 200 \times 10^6$ at/g observed at AM05 in the outflow area, and the core-top for RISP 79–14 at the rear of the Ross Ice Shelf (Sjunneskog et al., 2007) may approximate the lower range of ^{10}Be concentrations being deposited under modern Antarctic ice shelves.

This distribution of ^{10}Be, in combination with similar patterns for other proxies of sediment transport (diatoms & radiocarbon), provide support for the conceptual model that strong-bottom currents are a key process in determining ^{10}Be concentrations in sub-ice shelf environments.

5.2. Be isotopes as tracers of paleo-ice shelves and sub-ice shelf circulation

For ice-shelves with more limited sub-ice shelf current circulation and where current velocities are lower than needed for silt suspension and transport, the dilution of the ice shelf ^{10}Be signal may not be as significant as we observe in Prydz Bay. Hence, in those regions where advection is low and/or circulation does not transfer sediment from the ice shelf calving margin toward the grounding line, shifts in ^{10}Be concentrations through time may be representative of, and thus interpreted as, a change from sub-ice shelf to open marine settings (e.g. Yokoyama et al., 2016).

In contrast to the above, in regions with strong sub-ice shelf currents and sediment advection, it may not be possible to identify a specific ^{10}Be concentration (or range) that is unique to either open marine or sub-ice shelf settings. This is the case we observe in the Amery Ice Shelf – Prydz Bay data. In this case, the distribution of ^{10}Be is primarily affected by the strength and direction of sub-ice shelf circulation. Thus, there is potential for using ^{10}Be to identify whether or not changes in sub-shelf circulation have influenced paleo-ice sheet fluctuations.

Where strong sub-shelf circulations are present, the combination of both Be isotopes, in the Prydz Bay data, i.e. the ^{10}Be/^{9}Be ratio, appears to provide a better distinction between the three environments than ^{10}Be in isolation. Due to the lower 'reactive' ^{9}Be concentrations (i.e. HCl extractable) in open marine core top sediments, corresponding ^{10}Be/^{9}Be ratios are twice that of sub-ice shelf sediments, which in turn are five times larger than ratios in subglacial basal sediments. Moreover, the ^{10}Be/^{9}Be display less variability within each environment than either of the isotopes alone. We attribute both the spatial pattern and relatively low variability of ^{10}Be/^{9}Be to (a) input of ^{9}Be into the sub-ice shelf cavity from a terrestrial source (b) the long residence time of bottom waters (2 yr in the cavity) and potential for eddy circulation (Galton-Fenzi et al., 2012), which can thus produce a well-mixed water mass in the cavity, and (c) equilibration of the ^{10}Be/^{9}Be ratio characterizing the sediment source with the (dissolved) ^{10}Be/^{9}Be of the water column while the sediments are transported (e.g. Brown et al., 1992). Thus, the combination of the two process – mixing and equilibration – results in sediment ^{10}Be/^{9}Be ratios that are more homogeneous within each environment than across environments. This explains the consistency of ^{10}Be/^{9}Be within each of the three environments despite clearly far larger variability in ^{10}Be abundances. Thus, we conclude that ^{10}Be/^{9}Be ratios are a more

reliable tracer of sub-ice shelf settings than ^{10}Be concentrations, even in areas such as Prydz Bay where strong bottom currents advect significant amounts of ^{10}Be under the ice shelf.

5.3. Influence of ice sheets on global ocean $^{10/9}$Be ratios

Our ^{10}Be and ^{9}Be results from the Prydz Bay region add to knowledge of how glacial/interglacial cycles affect ^{10}Be/^{9}Be ratios in oceanic sediments (e.g. von Blanckenburg et al., 2015). Ice sheets collect their fluxes of ^{10}Be and ^{9}Be in a segregated way with little interaction prior to release at the ice sheet margin. The ^{10}Be flux is spread evenly throughout the ice (2–3 km thick in many locations), while the clear majority of the ^{9}Be is in sediment in the basal zone (lower few meters and the deforming bed). Compared to beryllium transport processes in terrestrial river catchments, there is practically no mixing of basal sediments and surface ice, and thus limited potential for equilibration of ^{10}Be/^{9}Be ratios during glacial transport to the grounding line and possibly also to the calving margin.

The separation of ^{10}Be and ^{9}Be fluxes during glacial transport also means that the two Be isotopes can be delivered to different terminal reservoirs in the glacio-marine system. Marine terminating ice sheets likely release their ^{9}Be flux largely near the grounding line – either due to melt out of subglacial sediment at the grounding line, or via subglacial drainage in meltwater channels. In contrast, ^{10}Be associated with glacial ice can melt out at the grounding line, but it can also be transported directly to the open marine setting through icebergs. This model allows Be-isotope mixing both in sub-ice shelf and open marine settings as shown in Fig. 1.

With the modern ice configuration (i.e. marine ice sheets with grounding lines several hundred kilometres from the continental shelf break), our results and others from Ross Sea indicate that decoupling of ^{10}Be and ^{9}Be fluxes occurs in a way that is significant for at least the local distribution of these isotopes. Today, around half the ice flux (and thus ^{10}Be) makes it off the continent as icebergs (Rignot and Jacobs, 2002), and half of that ends up crossing the continental shelf break to the open ocean beyond (Merino et al., 2016). This is substantially higher than the ∼6% of the terrestrially deposited ^{10}Be that reaches the global ocean via river sediments (von Blanckenburg and Bouchez, 2014). Conversely, there is little evidence to indicate that similar proportions of ^{9}Be reach the open ocean in the present ice sheet configuration. Much of the chemically available ^{9}Be (extracted by the aggressive HCl etch) appears to be trapped in the overdeepened troughs on the inner continental shelf. This process potentially occurs even in the Prydz Bay region, where strong sub-ice shelf currents circulate radiocarbon and ^{10}Be laden sediments into the sub-ice shelf cavity.

Our results provide evidence for the decoupling of ^{10}Be and ^{9}Be fluxes by ice sheets to the marine environment, but more work is needed before these results can be generalized for different ice configurations. For example, during stadials such as the Last Glacial Maximum, ice sheets in Antarctica and the northern hemisphere expanded across continental shelves. This expanded ice configuration means both ^{9}Be and ^{10}Be were transported at least as far as the continental shelf break. ^{10}Be concentrations and ^{10}Be/^{9}Be ratios in sediments deposited on the continental slope and rise adjacent to shelf-break glaciations in both Antarctica and the Arctic reduce during stadials compared to interstadials (Frank et al., 1995; Aldahan et al., 1997; Valetta et al., 2018). This temporal pattern is consistent with either increased export of mineral sediment and reactive ^{9}Be to the ice-sheet proximal deep ocean, and/or more long-distance dispersal of ^{10}Be by iceberg calving during continental shelf-break glaciations when compared to periods of reduced ice-sheet extent. However, substantial uncertainties remain in the source and rates of ^{10}Be redistribution around polar continental shelves (e.g. Frank et al., 1995; Valetta et al., 2018), and the pathways by which ^{9}Be sourced from sub-glacial terrigenous sediments is delivered to the open ocean during stadials. Thus, the role of ice sheet extent on transport of Be isotopes to the deep ocean need further work before the influence of ice sheet fluctuations on the global ^{10}Be/^{9}Be ratio is fully understood.

6. Conclusions

We find that Be isotope concentrations and their distributions in glacio-marine environments are more complex than previously reported. The variability in meteoric ^{10}Be and terrigenous ^{9}Be together with their spatial correlation within ice marginal marine deposits are a useful proxy of both sub-ice shelf circulation and of sediment depositional processes. ^{10}Be concentrations in Antarctic marine and glacial sediments are controlled by the source origin of those sediments. In modern Antarctic sediments, ^{10}Be largely follows the environmental setting, with typically decreasing concentrations from open marine, to sub-ice shelf, and finally subglacial. However, in some ice shelves, substantial long-distance transport of fine grained sediment via bottom currents into sub-ice shelf cavities means that the sediment deposited at a site may have been generated many hundreds of kilometres away. Thus, in these areas of strong sub-ice shelf circulation, bottom currents can potentially deposit sediment in a different environmental setting to its creation, and thus mix local values of ^{10}Be and ^{9}Be concentrations with both waters and sediment transported from a distant source of Be isotopes. In Prydz Bay and perhaps other ice-shelf settings, ^{10}Be/^{9}Be ratios, which are more strongly influenced by the water mass than the sediment, provide a more reliable measure of the depositional environment.

Acknowledgements

We thank Frank Krikowa for assistance with ICP-MS measurements, and acknowledge financial support for preparation and measurement of AMS targets through AINSE grant 11279 and ANSTO Research Portal Proposal 10713. AP publishes with the permission of the CEO, Geoscience Australia.

References

Aldahan, A.A., Ning, S., Possnert, G., Backman, J., Boström, K., 1997. ^{10}Be records from sediments of the Arctic Ocean covering the past 350 ka. Mar. Geol. 144 (1–3), 147–162.

Allison, Ian, 2003. The AMISOR project: ice shelf dynamics and ice–ocean interaction of the Amery Ice Shelf. FRISP Rep. 14, 74–82.

Beer, J., Bonani, G., Hofmann, H.J., Suter, M., Synal, A., Wölfli, W., Oeschger, H., Siegenthaler, U., Finkel, R.C., 1987. ^{10}Be measurements on polar ice: comparison of Arctic and Antarctic records. Nucl. Instrum. Methods Phys. Res., Sect. B, Beam Interact. Mater. Atoms 29 (1–2), 203–206.

Berkman, P.A., Forman, S.L., 1996. Pre-bomb radiocarbon and the reservoir correction for calcareous marine species in the Southern Ocean. Geophys. Res. Lett. 23 (4), 363–366.

Bourles, D., Raisbeck, G.M., Yiou, F., 1989. ^{10}Be and ^{9}Be in marine sediments and their potential for dating. Geochim. Cosmochim. Acta 53 (2), 443–452.

Brown, L., 1987. ^{10}Be as a tracer of erosion and sediment transport. Chem. Geol., Isot. Geosci. Sect. 65 (3–4), 189–196.

Brown, E.T., Edmond, J.M., Raisbeck, G.M., Bourlès, D.L., Yiou, F., 1992. Beryllium isotope geochemistry in tropical river basins. Geochim. Cosmochim. Acta 56 (4), 1607–1624.

Chmeleff, J., von Blanckenburg, F., Kossert, K., Jakob, D., 2010. Determination of the ^{10}Be half-life by multicollector ICP-MS and liquid scintillation counting. Nucl. Instrum. Methods Phys. Res., Sect. B, Beam Interact. Mater. Atoms 268 (2), 192–199.

Child, D., Elliot, G., Misfud, C., Smith, A.M., Fink, D., 2000. Sample processing for Earth science studies at ANTARES. Nucl. Instrum. Methods Phys. Res. B 172, 856–860.

Domack, E.W., Harris, P.T., 1998. A new depositional model for ice shelves, based upon sediment cores from the Ross Sea and the Mac. Robertson shelf, Antarctica. Ann. Glaciol. 27, 281–284.

Domack, E.W., Jull, A.J., Donahue, D.J., 1991. Holocene chronology for the unconsolidated sediments at hole 740A: Prydz Bay, East Antarctica. In: Barron, J., Larsen, B. (Eds.), Proceedings of the Ocean Drilling Program, Scientific Results, vol. 119, pp. 747–750.

Domack, E., O'Brien, P., Harris, P., Taylor, F., Quilty, P.G., De Santis, L., Raker, B., 1998. Late Quaternary sediment facies in Prydz Bay, East Antarctica and their relationship to glacial advance onto the continental shelf. Antarct. Sci. 10 (3), 236–246.

Fink, D., McKelvey, B., Hannan, D., Newsome, D., 2000. Cold rocks, hot sands: *in-situ* cosmogenic applications in Australia at ANTARES. Nucl. Instrum. Methods Phys. Res., Sect. B, Beam Interact. Mater. Atoms 172 (1–4), 838–846.

Fink, D., Smith, A., 2007. An inter-comparison of ^{10}Be and 26Al AMS reference standards and the ^{10}Be half-life. Nucl. Instrum. Methods Phys. Res., Sect. B, Beam Interact. Mater. Atoms 259 (1), 600–609.

Frank, M., Eisenhauer, A., Bonn, W.J., Walter, P., Grobe, H., Kubik, P.W., Dittrich-Hannen, B., Mangini, A., 1995. Sediment redistribution versus paleoproductivity change: Weddell Sea margin sediment stratigraphy and biogenic particle flux of the last 250,000 years deduced from ^{230}Th$_{ex}$, ^{10}Be and biogenic barium profiles. Earth Planet. Sci. Lett. 136 (3–4), 559–573.

Frank, M., Schwarz, B., Baumann, S., Kubik, P.W., Suter, M., Mangini, A., 1997. A 200 kyr record of cosmogenic radionuclide production rate and geomagnetic field intensity from ^{10}Be in globally stacked deep-sea sediments. Earth Planet. Sci. Lett. 149 (1–4), 121–129.

Fricker, H.A., Young, N.W., Allison, I., Coleman, R., 2002. Iceberg calving from the Amery ice shelf, East Antarctica. Ann. Glaciol. 34, 241–246.

Galton-Fenzi, B.K., Maraldi, C., Coleman, R., Hunter, J., 2008. The cavity under the Amery Ice Shelf, East Antarctica. J. Glaciol. 54 (188), 881–887.

Galton-Fenzi, B.K., Hunter, J.R., Coleman, R., Marsland, S.J., Warner, R.C., 2012. Modeling the basal melting and marine ice accretion of the Amery Ice Shelf. J. Geophys. Res., Oceans 117 (C9).

Graly, J.A., Corbett, L.B., Bierman, P.R., Lini, A., Neumann, T.A., 2018. Meteoric ^{10}Be as a tracer of subglacial processes and interglacial surface exposure in Greenland. Quat. Sci. Rev. 191, 118–131.

Guitard, M., 2015. Millennial-Scale Variability of a Major East Antarctic Outlet Glacier During the Last Glaciation. Masters Thesis. College of Marine Science, University of South Florida. http://scholarcommons.usf.edu/etd/5957.

Harris, P.T., Taylor, F., Pushina, Z., Leitchenkov, G., O'brien, P.E., Smirnov, V., 1998. Lithofacies distribution in relation to the geomorphic provinces of Prydz Bay, East Antarctica. Antarct. Sci. 10 (3), 227–235.

Hemer, M.A., Harris, P.T., 2003. Sediment core from beneath the Amery Ice Shelf, East Antarctica, suggests mid-Holocene ice-shelf retreat. Geology 31 (2), 127–130.

Hemer, M.A., Post, A.L., O'Brien, P.E., Craven, M., Truswell, E.M., Roberts, D., Harris, P.T., 2007. Sedimentological signatures of the sub-Amery Ice Shelf circulation. Antarct. Sci. 19 (4), 497–506.

Herraiz-Borreguero, L., Coleman, R., Allison, I., Rintoul, S.R., Craven, M., Williams, G.D., 2015. Circulation of modified Circumpolar Deep Water and basal melt beneath the Amery Ice Shelf, East Antarctica. J. Geophys. Res., Oceans 120 (4), 3098–3112.

Jenkins, A., Holland, D.M., Jacobs, S.S., 2003. Modelling the ocean circulation beneath the Ross Ice Shelf. Antarct. Sci. 15, 13–23.

Knudsen, M.F., Henderson, G.M., Frank, M., Mac Niocaill, C., Kubik, P.W., 2008. In-phase anomalies in Beryllium-10 production and palaeomagnetic field behaviour during the Iceland Basin geomagnetic excursion. Earth Planet. Sci. Lett. 265 (3), 588–599.

Larner, B.L., Seen, A.J., Palmer, A.S., Snape, I., 2007. A study of metal and metalloid contaminant availability in Antarctic marine sediments. Chemosphere 67 (10), 1967–1974.

Merino, N., Le Sommer, J., Durand, G., Jourdain, N.C., Madec, G., Mathiot, P., Tournadre, J., 2016. Antarctic icebergs melt over the Southern Ocean: climatology and impact on sea ice. Ocean Model. 104, 99–110.

Mikhalsky, E.V., Sheraton, J.W., Labia, A.A., Tingey, R.J., Thost, D.E., Kamenev, E.N., Fedorov, L.V., 2001. Geology of the Prince Charles Mountains, Antarctica. AGSO Bull. 247.

Mishra, D.C., Chandra Sekhar, D.V., Venkata Raju, D.C.H., Vijaya Kumar, V., 1999. Crustal structure based on gravity–magnetic modelling constrained from seismic studies under Lambert Rift, Antarctica and Godavari and Mahanadi rifts, India and their interrelationship. Earth Planet. Sci. Lett. 172, 287–300.

Nishiizumi, K., Imamura, M., Caffee, M.W., Southon, J.R., Finkel, R.C., McAninch, J., 2007. Absolute calibration of ^{10}Be. Nucl. Instrum. Methods Phys. Res., Sect. B, Beam Interact. Mater. Atoms 258, 403–413. Be AMS Standards.

Nunes Vaz, R.A., Lennon, G.W., 1996. Physical oceanography of the Prydz Bay region of Antarctic waters. Deep-Sea Res., Part 1, Oceanogr. Res. Pap. 43 (5), 603–641.

O'Brien, P.E., Harris, P.T., Quilty, P.G., Taylor, F., Wells, P., 1995. Post Cruise Report – Prydz Bay & Mac.Robertson Shelf, Antarctica. AGSO Record 1995/29.

Pavich, M.J., Brown, L., Klein, J., Middleton, R., 1984. ^{10}Be accumulation in a soil chronosequence. Earth Planet. Sci. Lett. 68 (2), 198–204.

Post, A.L., Galton-Fenzi, B.K., Riddle, M.J., Herraiz-Borreguero, L., O'Brien, P.E., Hemer, M.A., McMinn, A., Rasch, D., Craven, M., 2014. Modern sedimentation, circulation and life beneath the Amery Ice Shelf, East Antarctica. Cont. Shelf Res. 74, 77–87.

Pritchard, H.D., Ligtenberg, S.R.M., Fricker, H.A., Vaughan, D.G., van den Broeke, M.R., Padman, L., 2012. Antarctic ice-sheet loss driven by basal melting of ice shelves. Nature 484 (7395), 502–505.

Rignot, E., Jacobs, S.S., 2002. Rapid bottom melting widespread near Antarctic ice sheet grounding lines. Science 296 (5575), 2020–2023.

Scherer, R.P., Aldahan, A., Tulaczyk, S., Possnert, G., Engelhardt, H., Kamb, B., 1998. Pleistocene collapse of the West Antarctic ice sheet. Science 281 (5373), 82–85.

Sjunneskog, C., Scherer, R., Aldahan, A., Possnert, G., 2007. ^{10}Be in glacial marine sediment of the Ross Sea, Antarctica, a potential tracer of depositional environment and sediment chronology. Nucl. Instrum. Methods Phys. Res., Sect. B, Beam Interact. Mater. Atoms 259 (1), 576–583.

Taylor, F., Leventer, A., 2003. Late Quaternary palaeoenvironments in Prydz Bay, East Antarctica: interpretations from marine diatoms. Antarct. Sci. 15 (4), 512–521.

Taylor, F., McMinn, A., 2002. Late Quaternary diatom assemblages from Prydz bay, eastern Antarctica. Quat. Res. 57 (1), 151–161.

Valletta, R.D., Willenbring, J.K., Passchier, S., Elmi, C., 2018. ^{10}Be/^{9}Be ratios reflect Antarctic Ice Sheet freshwater discharge during Pliocene warming. Paleoceanogr. Paleoclimatol. https://doi.org/10.1029/2017PA003283.

von Blanckenburg, F., Bouchez, J., 2014. River fluxes to the sea from the ocean's ^{10}Be/^{9}Be ratio. Earth Planet. Sci. Lett. 387, 34–43.

von Blanckenburg, F., Bouchez, J., Wittmann, H., 2012. Earth surface erosion and weathering from the ^{10}Be (meteoric)/^{9}Be ratio. Earth Planet. Sci. Lett. 351, 295–305.

von Blanckenburg, F., Bouchez, J., Ibarra, D.E., Maher, K., 2015. Stable runoff and weathering fluxes into the oceans over Quaternary climate cycles. Nat. Geosci. 8 (7), 538.

White, D.A., Fink, D., Gore, D.B., 2011. Cosmogenic nuclide evidence for enhanced sensitivity of an East Antarctic ice stream to change during the last deglaciation. Geology 39 (1), 23–26.

Willenbring, J.K., von Blanckenburg, F., 2010. Meteoric cosmogenic Beryllium-10 adsorbed to river sediment and soil: applications for Earth-surface dynamics. Earth-Sci. Rev. 98 (1–2), 105–122.

Williams, G.D., Herraiz-Borreguero, L., Roquet, F., Tamura, T., Ohshima, K.I., Fukamachi, Y., Fraser, A.D., Gao, L., Chen, H., McMahon, C.R., et al., 2016. The suppression of Antarctic bottom water formation by melting ice shelves in Prydz Bay. Nat. Commun. 7 (6), 12577.

Wittmann, H., Blanckenburg, F., Bouchez, J., Dannhaus, N., Naumann, R., Christl, M., Gaillardet, J., 2012. The dependence of meteoric ^{10}Be concentrations on particle size in Amazon River bed sediment and the extraction of reactive ^{10}Be/^{9}Be ratios. Chem. Geol. 318, 126–138.

Yokoyama, Y., Anderson, J.B., Yamane, M., Simkins, L.M., Miyairi, Y., Yamazaki, T., Koizumi, M., Suga, H., Kusahara, K., Prothro, L., Hasumi, H., 2016. Widespread collapse of the Ross Ice Shelf during the late Holocene. Proc. Natl. Acad. Sci. USA 113 (9), 2354–2359.

Yu, J., Liu, H., Jezek, K.C., Warner, R.C., Wen, J., 2010. Analysis of velocity field, mass balance, and basal melt of the Lambert Glacier–Amery Ice Shelf system by incorporating 80 Radarsat SAR interferometry and ICESat laser altimetry measurements. J. Geophys. Res., Solid Earth 115 (11), 1–16.